Electronic Supplementary Material (ESI) for Physical Chemistry Chemical Physics.

ELECTRONIC SUPPLEMENTARY INFORMATION

A Quest for Ideal Electric Field-Driven MX@C_{70} Endohedral Fullerene Memristors: Which MX Fits the Best?

Lucie Tučková,[1,2] Adam Jaroš,[1,3] Cina Foroutan-Nejad,[1,4*] Michal Straka[1*]

[1]Institute of Organic Chemistry and Biochemistry of the Czech Academy of Sciences, Flemingovo nám. 2, CZ–16610, Prague, Czech Republic
[2]Faculty of Chemical Engineering, University of Chemistry and Technology Prague, Technická 3, CZ–16628, Prague, Czech Republic
[3]Faculty of Science, Charles University, Albertov 2038/6, CZ–12843, Prague, Czech Republic
[4]Institute of Organic Chemistry, Polish Academy of Sciences, Kasprzaka 44/52, 01-224, Warsaw, Poland

Stability of endo- versus endo-exofullerene $NaClC_{70}$

The system with the molecular formula of $NaClC_{70}$ was optimized in the endofullerene $NaCl@C_{70}$ geometry and several endo-exofullerene $Na@C_{70}$-Cl isomers as shown in **Figure S1**. The relative energies of the geometries optimized at the PBE0-D3/def2-SVP level are listed in **Table S1**. The effect of stabilization of the $Na@C_{70}$-Cl species via charge transfer between the metal and the cage proposed by a referee does not take place, as the endohedral species is found to be more stable by at least 44.6 kcal/mol.

Table S1: Energies of different $NaClC_{70}$ isomers optimized at the PBE0-D3/def2-SVP level relative to the lowest energy found (ΔE in kcal/mol).

isomer	ΔE
$NaCl@C_{70}$	0.0
$Na@C_{70}$-Cl(α)	44.6
$Na@C_{70}$-Cl(β)	50.2
$Na@C_{70}$-Cl(γ)	47.4
$Na@C_{70}$-Cl(δ)	47.5
$Na@C_{70}$-Cl(ε)	57.1

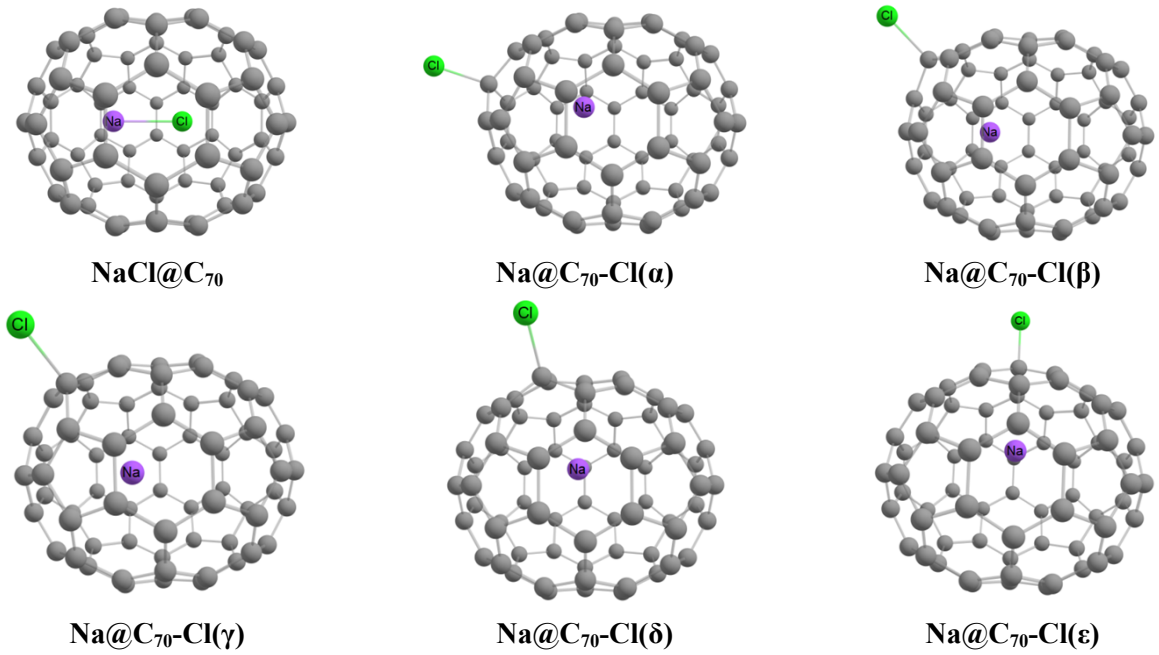

Figure S1: Optimized structures of different $NaClC_{70}$ isomers.

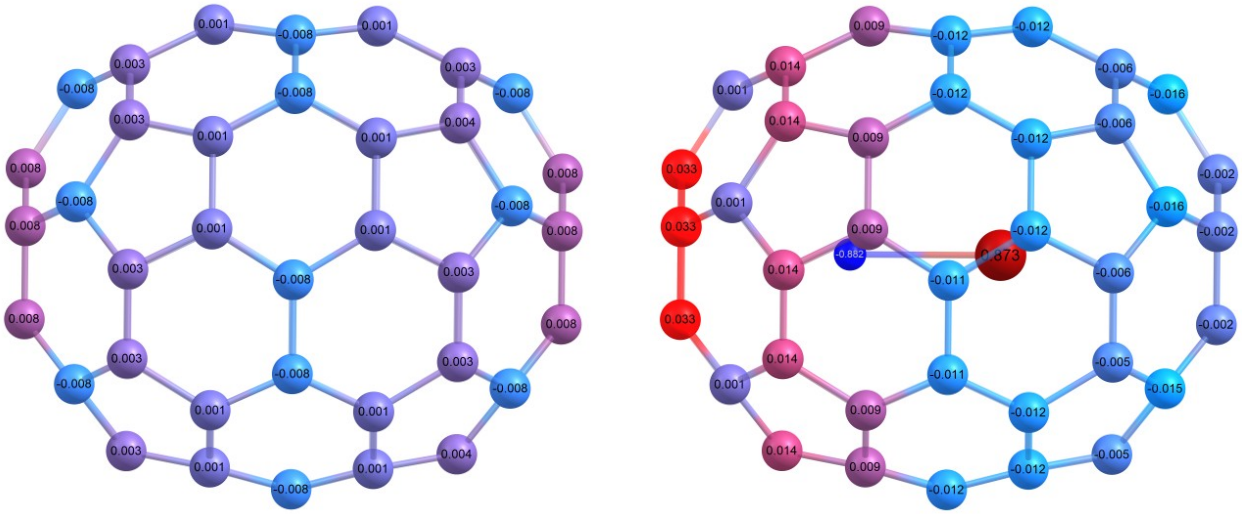

a **b**

Figure S2: Charges obtained from natural population analysis (NPA) of (**a**) C_{70} and (**b**) $KF@C_{70}$ systems.

Basis set convergence at the *ab initio* level

Table S1 reveals fast convergence of ISB with the basis set, within 1 kcal/mol already with the def2-TZVP basis set. The larger def2-QZVP basis set only presents a marginal improvement. Hence, the def2-TZVP basis set can be considered as converged for the calculations of the

intrinsic switching barrier in MX@C_n systems. Note that even the small def2-SVP basis set already provides barriers within 1–2 kcal/mol from the largest def2-QZVP basis set. The fast convergence can be easily understood – here we subtract energies of two rather similar systems (LM and TS) of a particular molecule which means significant error cancellation for any level applied. For the same reason, it is not necessary to apply the complete basis set (CBS) extrapolation.

The basis set convergence of SCS-MP2 encapsulation energy (**Table S2**) is not as smooth as for ISB, particularly when the BSSE is omitted. Even with the BSSE (counterpoise) correction included in EE_{BSSE}, results are not satisfactorily converged. Hence, we employed Helgaker's extrapolation formula(1) for the calculation of the energies at the CBS limit. The absolute difference between the BSSE-corrected and uncorrected EEs for the various basis sets is then between 22–43 kcal/mol for def2-SVP, 7–18 kcal/mol for def2-TZVP, 3–12 kcal/mol for def2-QZVP, and 0.1–9 kcal/mol for the CBS.

Table S2: Switching barriers (in kcal/mol) of the test set MX@C_{70} systems calculated using SCS-MP2 and different basis sets. The molecular geometries were optimized at the B97D3/def2-SVP level; the def2-QZVPP cbas auxiliary basis set was used for Zn and Cu atoms.

MX →	KF	CsF	LiCl	CuCl	ZnS
def2-SVP	13.9	41.7	0.1	2.1	4.6
def2-TZVP	10.9	42.2	-1.2	1.5	2.8
def2-QZVP	10.0	41.6	-1.2	1.0	1.9

Table S3: Encapsulation energies (in kcal/mol) of the test set MX@C_{70} systems calculated using SCS-MP2 with different basis sets and the complete basis set extrapolation (CBS). The molecular geometries were optimized at the B97D3/def2-SVP level; the def2-QZVPP cbas auxiliary basis set was used for Zn and Cu atoms. BSSE-uncorrected values are in columns denoted as un., corrected values are in columns denoted as corr.

MX →	KF		CsF		LiCl		CuCl		ZnS	
	un.	corr.	un.	corr.	un.	corr.	un.	corr.	un.	corr.
def2-SVP	-51.2	-16.2	-55.9	-14.5	-39.7	-17.3	-58.9	-16.0	-63.4	-21.1
def2-TZVP	-31.8	-23.5	-45.1	-26.8	-34.8	-28.0	-46.4	-30.3	-54.8	-39.3
def2-QZVP	-33.1	-25.5	-43.5	-31.0	-33.0	-29.9	-40.7	-34.6	-49.2	-43.4
CBS	-35.2	-27.1	-42.6	-33.8	-32.3	-31.0	-38.2	-37.7	-45.9	-46.0

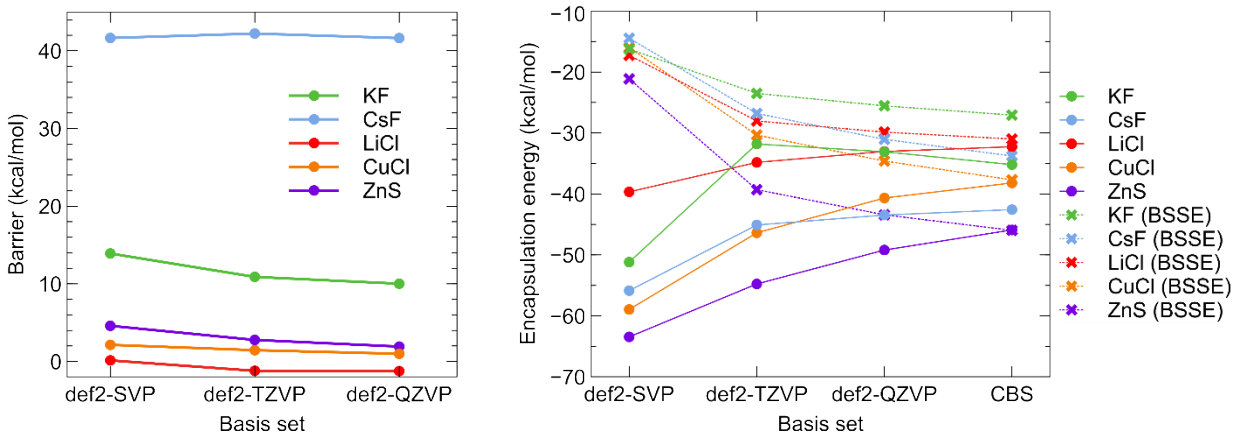

a **b**

Figure S3: (**a**) Basis set convergence for the intrinsic switching barrier of the test set MX@C_{70} systems calculated using the SCS-MP2 method; (**b**) basis set convergence of the encapsulation energy with and without the BSSE correction calculated using the SCS-MP2 method. The complete basis set extrapolation (CBS) results are shown for encapsulation energy in (**b**).

Table S4: The intrinsic switching barrier (in kcal/mol) of the test set MX@C_{70} compounds calculated at different levels using the PBE0-D3/def2-SVP optimized structures. The RMSE was calculated using the DLPNO-CCSD(T) values as the reference.

MX →	KF	CsF	LiCl	CuCl	ZnS	RMSE
SCS-MP2/def2-TZVP	19.0	42.2	2.4	1.0	3.4	1.7
DLPNO-CCSD(T)/def2-TZVP	19.9	43.6	1.8	4.0	4.8	–
PBE0/def2-SVP	18.2	38.8	3.3	5.2	6.8	2.6
PBE0 /def2-TZVP	18.5	38.9	2.0	2.9	4.3	2.3

Table S5: The intrinsic switching barrier (in kcal/mol) of the test set MX@C_{70} compounds calculated at different DFT-D3 levels employing structures optimized at the appertaining levels.

MX →	KF	CsF	LiCl	CuCl	ZnS
B97D3/def2-SVP	16.6	33.3	10.4	9.3	11.8
B97D3/def2-TZVP	15.2	34.5	8.6	7.8	10.3
B97D3/def2-QZVP	14.8	33.8	8.7	7.9	10.2
TPSS/def2-SVP	17.0	35.5	3.4	1.3	6.9
TPSS/def2-TZVP	16.5	35.1	1.8	-0.8	4.6
TPSS/def2-QZVP	16.2	34.5	1.8	-1.1	4.4

Table S6: The encapsulation energies (in kcal/mol) of the test set MX@C_{70} compounds calculated at different DFT-D3 levels. Calculated using structures of MX@C_{70} and the free MX and C_{70} optimized at the appertaining levels.

MX →	KF	CsF	LiCl	CuCl	ZnS
B97D3/def2-SVP	-20.6	26.5	-45.7	-60.0	-56.2
B97D3/def2-TZVP	-2.5	41.4	-35.6	-41.3	-37.2
B97D3/def2-QZVP	0.0	41.6	-34.0	-37.9	-35.5
TPSS/def2-SVP	-42.5	-27.0	-40.5	-57.6	-59.3
TPSS/def2-TZVP	-25.5	-10.2	-29.5	-37.1	-37.7
TPSS/def2-QZVP	-23.1	-10.2	-28.3	-33.5	-36.0

Table S7: The basis set superposition error (BSSE)-corrected encapsulation energies (in kcal/mol) of the test set MX@C_{70} compounds calculated using the two DFT-D3 functionals. Calculated using structures of MX@C_{70} optimized at the DFT-D3/def2-SVP level.

MX →	KF	CsF	LiCl	CuCl	ZnS
B97D3/def2-SVP	-2.2	43.5	-34.2	-35.9	-33.5
B97D3/def2-TZVP	-2.8	43.9	-34.2	-37.2	-35.0
B97D3/def2-QZVP	-3.1	42.4	-34.7	-37.9	-36.1
TPSS/def2-SVP	-22.9	-10.1	-29.1	-33.0	-35.3
TPSS/def2-TZVP	-22.7	-8.2	-28.4	-33.2	-35.4
TPSS/def2-QZVP	-22.9	-9.4	-28.8	-33.4	-36.2

Table S8: The encapsulation energies (in kcal/mol) of the test set MX@C_{70} compounds calculated at different DFT-D3 levels using the def2-TZVP basis set; SVP denotes the geometries optimized at the DFT-D3/def2-SVP level and TZVP denotes the geometries optimized at the DFT-D3/def2-TZVP level.

MX →	KF		CsF		LiCl		CuCl		ZnS	
	SVP	TZVP	SVP	TZVP	SVP	TZVP	SVP	TZVP	SVP	TZVP
B97D3	-2.7	-2.5	41.5	41.4	-35.7	-35.6	-41.5	-41.3	-37.5	-37.2
TPSS	-25.7	-25.5	-10.1	-10.2	-30.1	-29.5	-37.2	-37.1	-37.9	-37.7

Table S9: Root-mean-square differences of atomic positions (RMSDs in Å) of the test set MX@C_{70} systems LM and TS structures optimized using two DFT-D3 functionals and the def2-SVP basis set with respect to the geometries optimized at the DFT-D3/def2-TZVP level.

MX →	KF		CsF		LiCl		CuCl		ZnS	
	LM	TS	LM	TS	LM	TS	LM	TS	LM	TS
B97D3	0.024	0.018	0.018	0.024	0.017	0.023	0.016	0.016	0.016	0.016
TPSS	0.025	0.018	0.018	0.018	0.136	0.021	0.017	0.016	0.016	0.016

Table S10: SCS-MP2/def2-TZVP single-point energies (in kcal/mol) of DFT-D3/def2-SVP-optimized geometries relative to the energies of the SCS-MP2/def2-TZVP-optimized geometries.

MX →	KF		CsF		LiCl		CuCl		ZnS	
	LM	TS	LM	TS	LM	TS	LM	TS	LM	TS
SCS-MP2	0.0	0.0	0.0	0.0	0.0	0.0	0.0	0.0	0.0	0.0
PBE0	3.2	1.8	1.8	1.7	1.8	1.5	1.9	1.5	1.8	1.7
M06	3.5	2.1	1.7	1.6	1.8	1.6	1.7	1.7	2.0	1.8
TPSSh	5.0	2.1	2.1	2.1	3.5	1.5	1.8	1.4	1.8	1.7
B3LYP	6.9	3.0	3.8	3.3	4.6	2.4	4.2	2.7	4.3	3.0
TPSS	7.8	4.4	4.5	4.8	3.7	3.6	3.6	3.9	3.9	3.9
PBE	6.8	5.3	5.8	5.9	5.2	4.7	4.9	5.2	5.2	5.2
ωB97X	6.7	5.9	5.7	6.0	7.0	5.5	6.6	5.9	6.8	6.2
BHLYP	8.0	6.1	6.3	5.7	7.1	5.7	6.8	6.2	6.7	5.9
B97D3	18.0	8.4	8.7	8.7	10.9	7.0	7.4	7.5	8.6	7.9
BLYP	20.2	13.8	15.5	15.3	14.7	12.1	14.4	12.8	14.7	13.3

In the following tables, the functionals were sorted by the value of the root-mean-square error (RMSE) which was calculated according to the following formula:

$$RMSE = \sqrt{\frac{\sum_{N}(R_{DFT} - R_{MP2})^2}{N}}$$

where R_{DFT} is the observed parameter from the DFT-optimized geometries, R_{MP2} is the same parameter from the reference SCS-MP2-optimized geometries, and N is the number of molecules.

Table S11: M–X bond length (in pm) of the test set MX@C_{70} systems LM structures optimized using various DFT-D3 functionals with the def2-SVP basis set, and the reference SCS-MP2/def2-TZVP method.

MX →	KF	CsF	LiCl	CuCl	ZnS	RMSE
SCS-MP2	**232.5**	**246.8**	**213.4**	**212.5**	**209.3**	
M06	224.1	243.9	210.7	213.1	206.6	4.3
PBE	223.6	243.0	210.3	212.5	207.5	4.6
ωB97X	223.6	242.7	209.4	211.6	205.1	5.1
PBE0	222.8	242.1	209.4	212.5	206.9	5.3
TPSS	221.5	243.6	209.2	212.4	207.4	5.5
TPSSh	221.5	242.9	209.1	212.4	207.2	5.6
BHLYP	220.7	240.0	207.4	212.8	206.0	6.8
B3LYP	219.4	240.6	206.5	211.1	206.3	7.3
BLYP	218.5	241.4	205.9	210.2	206.7	7.7
B97D3	217.2	241.8	206.5	212.1	207.0	7.9

Table S12: Distance (in pm) of the uttermost pentagons of the fullerene (longest C–C distance) of the test set MX@C_{70} systems LM structures and the empty C_{70} optimized using various DFT-D3 functionals with the def2-SVP basis set, and the reference SCS-MP2/def2-TZVP method.

MX →	KF	CsF	LiCl	CuCl	ZnS	C_{70}	RMSE
SCS-MP2	**792.5**	**794.9**	**790.9**	**790.9**	**789.4**	**791.8**	
M06	793.1	794.8	792.0	790.3	790.4	792.0	0.8
PBE0	793.1	795.0	791.6	791.9	791.2	792.2	1.0
BHLYP	791.7	793.4	790.1	791.0	790.2	790.4	1.1
TPSSh	796.0	797.2	794.5	794.0	793.6	794.6	3.6
ωB97X	795.9	798.1	795.2	795.2	794.6	795.2	4.4
B3LYP	797.1	798.3	795.0	795.4	795.0	795.1	4.7
TPSS	798.0	799.1	796.1	795.4	795.5	796.5	5.6
PBE	798.0	799.9	796.5	795.5	796.0	797.1	6.0
B97D3	800.7	800.8	799.2	798.2	798.2	797.8	8.2
BLYP	802.8	803.4	800.3	800.4	800.1	800.2	10.4

Table S13: Root-mean-square differences of atomic positions (RMSDs in Å) of the test set MX@C_{70} systems LM structures and the empty C_{70} geometries optimized using various DFT-D3 functionals with the def2-SVP basis set with respect to the LM geometries optimized at the reference SCS-MP2/def2-TZVP level. The functionals are sorted by the sum of all the RMSD values obtained for each functional from the lowest to the highest.

MX →	KF	CsF	LiCl	CuCl	ZnS	C_{70}
PBE0	0.037	0.014	0.027	0.020	0.029	0.007
M06	0.040	0.014	0.030	0.036	0.025	0.009
TPSSh	0.051	0.018	0.099	0.018	0.030	0.010
TPSS	0.055	0.026	0.082	0.021	0.034	0.021
ωB97X	0.035	0.018	0.104	0.032	0.055	0.015
PBE	0.043	0.029	0.099	0.028	0.037	0.024
BHLYP	0.047	0.026	0.090	0.040	0.057	0.020
B3LYP	0.056	0.025	0.092	0.040	0.058	0.012
B97D3	0.080	0.030	0.104	0.036	0.058	0.028
BLYP	0.076	0.048	0.106	0.054	0.067	0.039

Table S14: M–X bond length (in pm) of the test set MX@C_{70} systems TS structures optimized using various DFT-D3 functionals with the def2-SVP basis set, and the reference SCS-MP2/def2-TZVP method.

MX →	KF	CsF	LiCl	CuCl	ZnS	RMSE
SCS-MP2	**217.2**	**228.1**	**205.3**	**206.2**	**203.7**	
PBE	217.2	228.1	205.3	206.2	203.7	1.7
M06	215.3	229.5	203.5	208.3	202.5	1.7
TPSS	214.7	226.9	203.7	207.6	202.0	1.9
TPSSh	214.7	229.3	203.4	208.2	202.0	2.1
PBE0	213.9	228.1	203.3	207.8	201.7	2.4
BLYP	213.4	226.8	202.8	207.2	201.5	2.5
B97D3	213.5	228.5	201.9	207.1	201.5	2.5
B3LYP	213.8	230.5	202.7	207.0	201.2	3.0
ωB97X	212.5	226.5	201.8	206.5	201.0	3.1
BHLYP	212.7	225.9	202.0	206.3	200.1	3.8

Table S15: Distance (in pm) of the uttermost pentagons of the fullerene (longest C–C distance) of the test set MX@C_{70} systems TS structures optimized using various DFT-D3 functionals with the def2-SVP basis set, and the reference SCS-MP2/def2-TZVP method.

MX →	KF	CsF	LiCl	CuCl	ZnS	RMSE
SCS-MP2	**788.1**	**785.5**	**789.8**	**789.4**	**788.7**	
BHLYP	787.4	785.4	789.2	787.9	786.9	1.1
PBE0	789.5	787.4	791.0	790.3	789.1	1.3
M06	789.5	787.0	791.2	790.3	789.7	1.3
TPSSh	791.8	789.9	793.3	792.7	791.3	3.5
ωB97X	791.0	790.0	793.6	792.8	791.8	3.6
B3LYP	791.9	790.4	793.8	792.7	791.4	3.8
TPSS	793.7	792.0	795.1	794.6	793.2	5.5
PBE	794.4	792.5	795.8	795.3	794.1	6.2
B97D3	795.0	793.9	796.1	795.6	794.0	6.7
BLYP	796.8	796.0	798.7	797.8	796.2	8.8

Table S16: Root-mean-square differences of atomic positions (RMSDs in Å) of the test set MX@C_{70} systems TS structures optimized using various DFT-D3 functionals with the def2-SVP basis set with respect to the TS geometries optimized at the reference SCS-MP2/def2-TZVP level. The functionals are sorted by the sum of all the RMSD values obtained for each functional from the lowest to the highest.

MX →	KF	CsF	LiCl	CuCl	ZnS
PBE0	0.125	0.011	0.009	0.009	0.010
ωB97X	0.125	0.017	0.015	0.017	0.016
B3LYP	0.126	0.019	0.014	0.016	0.016
BHLYP	0.126	0.020	0.020	0.025	0.021
M06	0.146	0.017	0.010	0.008	0.034
TPSS	0.128	0.026	0.021	0.024	0.023
PBE	0.127	0.029	0.026	0.027	0.026
B97D3	0.129	0.034	0.030	0.030	0.043
BLYP	0.133	0.046	0.040	0.041	0.041
TPSSh	0.126	0.016	0.012	0.223	0.014

Table S17: M–X bond length (in pm) of the test set MX@C_{70} systems LM structures optimized using various DFT-D3 functionals with different basis sets (SVP denotes the def2-SVP and TZVP the def2-TZVP basis set).

MX →	KF	CsF	LiCl	CuCl	ZnS
SCS-MP2	**232.5**	**246.8**	**213.4**	**212.5**	**209.3**
PBE0/SVP	222.8	242.1	209.4	212.5	206.9
PBE0/TZVP	224.4	239.2	209.5	209.6	206.1
B97D3/SVP	217.2	241.8	206.5	212.1	207.0
B97D3/TZVP	217.7	243.4	205.2	208.6	205.4
TPSS/SVP	221.5	243.6	209.2	212.4	207.4
TPSS/TZVP	223.5	241.6	210.4	209.1	206.2

Table S18: Distance (in pm) of the uttermost pentagons of the fullerene (longest C–C distance) of the test set MX@C_{70} systems LM structures optimized using three DFT-D3 functionals with different basis sets (SVP denotes the def2-SVP and TZVP the def2-TZVP basis set).

MX →	KF	CsF	LiCl	CuCl	ZnS	C_{70}
SCS-MP2	**792.5**	**794.9**	**790.9**	**790.9**	**789.4**	**791.8**
PBE0/SVP	793.1	795.0	791.6	791.9	791.2	792.2
PBE0/TZVP	789.5	791.5	787.9	788.2	787.4	788.7
B97D3/SVP	800.7	800.8	799.2	798.2	798.2	797.8
B97D3/TZVP	796.8	796.1	795.7	794.4	794.5	794.1
TPSS/SVP	798.0	799.1	796.1	795.4	795.5	796.5
TPSS/TZVP	793.9	795.4	792.3	791.6	791.8	792.8

Table S19: Root-mean-square differences of atomic positions (RMSDs in Å) of the test set MX@C_{70} systems LM structures and the empty C_{70} geometries optimized using various DFT-D3 functionals with the def2-SVP (denoted as SVP) or the def2-TZVP (denoted as TZVP) basis set with respect to the LM geometries optimized at the reference SCS-MP2/def2-TZVP level.

MX →	KF	CsF	LiCl	CuCl	ZnS	C_{70}
PBE0/SVP	0.037	0.014	0.027	0.020	0.029	0.007
PBE0/TZVP	0.027	0.023	0.021	0.022	0.033	0.022
B97D3/SVP	0.080	0.030	0.104	0.036	0.058	0.028
B97D3/TZVP	0.061	0.014	0.105	0.025	0.055	0.011
TPSS/SVP	0.055	0.026	0.082	0.021	0.034	0.021
TPSS/TZVP	0.033	0.011	0.099	0.011	0.028	0.005

Table S20: Intrinsic switching barriers calculated using different DFT-D3/def2-SVP levels (columns denoted as DFT) and the SCS-MP2/def2-TZVP single-point energies of the DFT-D3/def2-SVP-optimized structures (columns denoted as MP2; all in kcal/mol).

MX →	KF		CsF		LiCl		CuCl		ZnS		RMSE
	DFT	MP2	DFT	MP2	DFT	MP2	DFT	MP2	DFT	MP2	
M06	16.1	19.0	39.9	42.1	3.6	2.5	-0.2	1.5	2.2	3.2	1.9
PBE0	18.2	19.0	38.8	42.2	3.3	2.4	5.2	1.0	6.8	3.4	2.9
TPSSH	17.8	17.5	37.0	42.3	3.5	0.8	3.6	1.1	7.5	3.4	3.4
TPSS	17.0	17.0	35.5	42.5	3.4	2.7	1.3	1.7	6.9	3.5	3.5
PBE	16.4	19.0	35.3	42.4	2.1	2.2	-0.6	1.7	5.0	3.4	3.6
ωB97X	20.5	19.6	44.2	42.5	5.6	1.3	9.9	0.7	8.3	2.9	5.2
B3LYP	19.8	16.5	38.5	41.7	3.2	0.6	9.3	-0.1	10.2	2.1	6.0
BLYP	19.6	14.0	34.9	42.0	3.6	0.2	7.1	-0.2	10.8	2.1	6.7
BHLYP	20.8	18.6	42.8	41.6	3.5	1.4	13.5	0.7	10.6	2.6	6.9
B97D3	16.6	10.9	36.4	42.2	10.4	-1.2	9.3	1.5	11.7	2.8	8.3

Table S21: Encapsulation energies calculated using different DFT-D3/def2-TZVP methods (columns denoted as DFT) and SCS-MP2/def2-TZVP (counterpoise-corrected) single-point energies of the DFT-D3/def2-SVP-optimized structures (columns denoted as MP2; all in kcal/mol).

MX →	KF		CsF		LiCl		CuCl		ZnS		RMSE
	DFT	MP2	DFT	MP2	DFT	MP2	DFT	MP2	DFT	MP2	
M06	-34.1	-27.2	-22.0	-26.0	-35.4	-31.4	-36.9	-29.6	-34.1	-39.4	5.7
PBE0	-27.4	-27.4	-12.5	-26.0	-28.2	-31.2	-32.4	-30.1	-32.9	-39.4	6.9
TPSSH	-27.3	-26.3	-13.0	-26.5	-29.4	-29.7	-37.7	-30.4	-39.4	-39.8	6.9
BHLYP	-31.6	-26.4	-13.5	-24.9	-28.9	-29.7	-33.6	-29.1	-29.7	-38.3	7.1
TPSS	-25.7	-26.3	-10.1	-27.1	-30.1	-31.4	-37.2	-30.7	-37.9	-40.1	8.2
B3LYP	-31.4	-25.7	-10.7	-26.2	-30.5	-29.3	-36.1	-29.3	-30.9	-38.8	8.7
ωB97X	-39.5	-27.7	-27.5	-26.1	-38.9	-29.8	-46.5	-28.2	-45.4	-38.4	11.0
BLYP	-30.9	-25.0	-5.5	-27.4	-32.9	-29.3	-37.9	-29.6	-31.5	-39.4	11.5
PBE	-23.9	-27.8	-5.7	-27.3	-25.6	-31.3	-28.1	-30.6	-25.7	-40.2	12.1
B97D3	-2.7	-23.5	41.5	-26.8	-35.7	-28.0	-41.5	-30.3	-37.5	-39.3	32.5

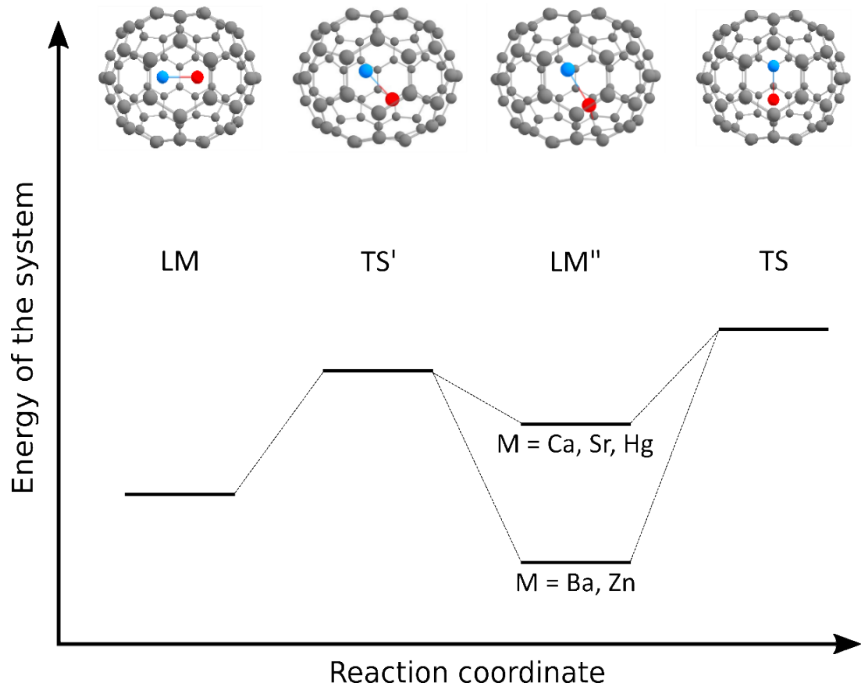

Figure S4: A schematical representation of the potential energy surface (PES) of MO@C_{70} (M = Ca, Sr, Ba, Zn, Hg) with the usual local minimum (LM), additional transition state (TS'), additional local minimum (LM''), and the transition state (TS). Oxygen atom is in red, metal atom is in blue.

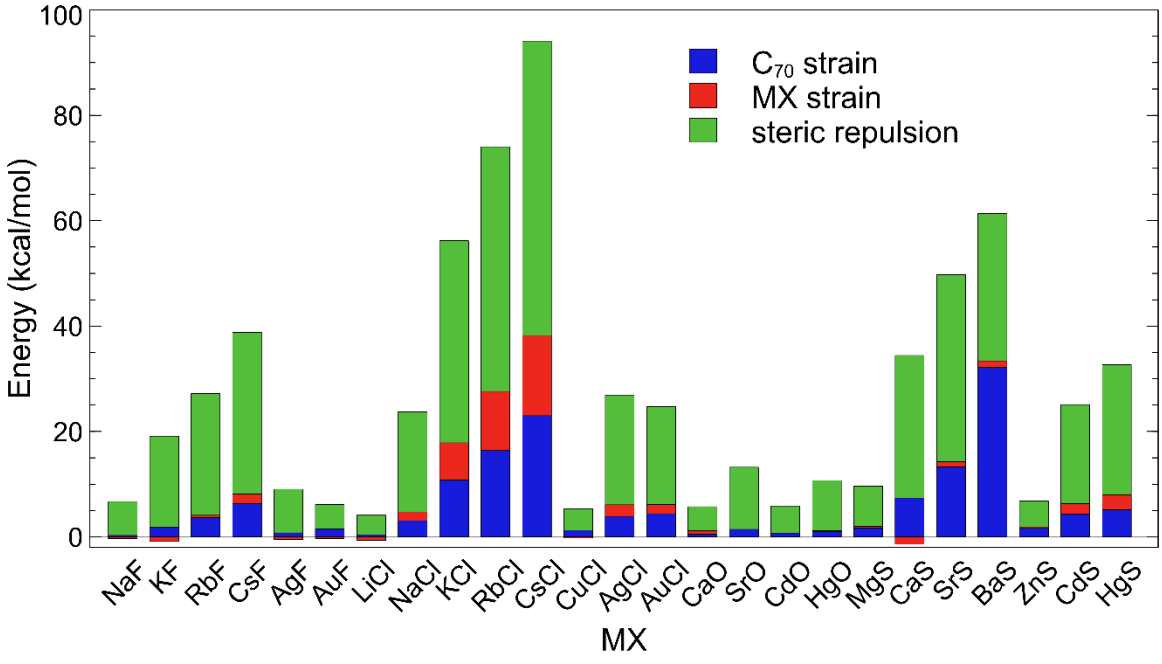

Figure S5: Contributions to intrinsic switching barriers divided into steric repulsion, and strain of MX and C_{70}, which was calculated as the difference between the energy of the MX/C_{70} in the TS and LM geometries.

Table S22: Properties of MX@C_{70} systems and the free MX: M–X bond lengths ($r_{M–X}$), dipole moments (μ), and encapsulation energies (EE); calculated at the PBE0-D3/def2-SVP level (EEs calculated with the def2-TZVP basis set as described in the main text).

MX	$r_{M–X}$ in MX@C_{70} (pm)	$r_{M–X}$ in MX (pm)	μ in MX@C_{70} (Debye)	μ in MX (Debye)	EE (kcal/mol)
NaF	194.8	188.9	2.00	7.32	-31.7
KF	222.8	214.0	2.21	7.79	-27.4
RbF	235.4	230.1	2.39	8.42	-23.2
CsF	242.1	239.4	2.29	7.69	-12.5
AgF	202.6	197.4	1.70	5.33	-32.6
AuF	197.5	193.5	1.34	4.02	-30.4
LiCl	208.9	200.4	1.76	6.59	-28.5
NaCl	237.0	234.0	2.32	8.22	-27.0
KCl	257.5	265.8	2.50	9.61	-11.6
RbCl	264.7	281.9	2.53	10.36	4.4
CsCl	269.4	294.1	2.46	9.96	26.0
CuCl	212.5	208.3	1.72	5.33	-32.4
AgCl	228.6	230.2	1.84	5.32	-24.8
AuCl	223.1	225.4	1.42	3.61	-23.0
CaO	185.9	180.3	2.65	8.40	-37.7
SrO	199.9	195.2	2.96	8.65	-34.1
CdO	191.1	189.4	2.01	5.42	-33.1
HgO	191.6	190.6	1.61	4.48	-36.4
MgS	218.0	215.7	3.24	7.51	-40.9
CaS	239.5	229.9	3.45	9.92	-37.6
SrS	250.3	244.9	3.60	10.37	-25.0
BaS	256.1	257.5	3.41	10.29	-4.5
ZnS	206.9	205.4	2.42	5.83	-32.8
CdS	222.3	224.6	2.44	5.61	-24.1
HgS	221.8	227.5	1.80	4.40	-24.9

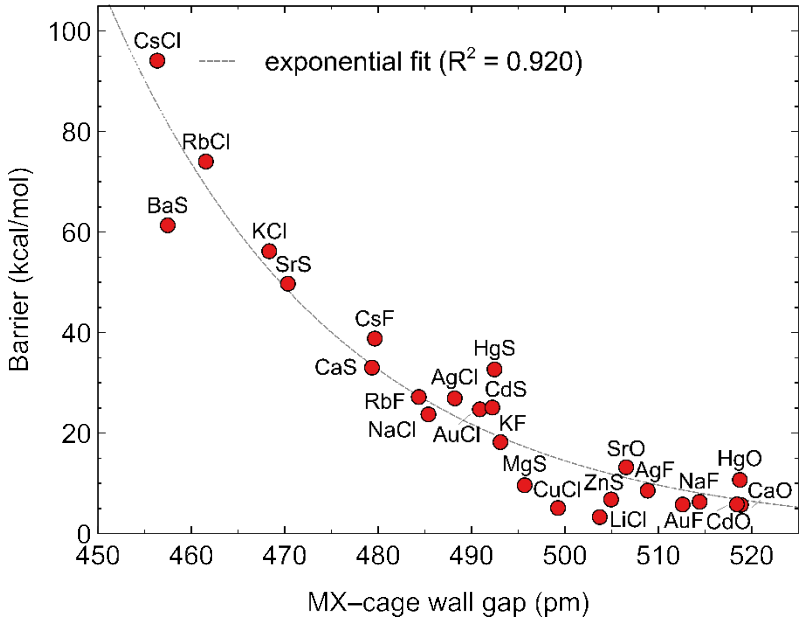

Figure S6: The correlation between the intrinsic switching barrier the difference of the empty C_{70} cage width and the M–X bond length in the TS geometry (MX–cage wall gap).

Table S23: Switching barriers calculated employing total energies (SB_0) and enthalpies at 298.15 K (SB_{298}, both in kcal/mol) for denoted MX@C_{70} systems at different electric fields (EF in V/Å).

EF →	0.00		0.21		0.41		0.62		0.82		1.03	
MX	SB_0	SB_{298}	SB_0	SB_{298}	SB_0	SB_{298}	SB_0	SB_{298}	SB_0	SB_{298}	SB_0	SB_{298}
NaF	6.3	5.6	3.8	4.5	2.2	2.8	0.9	1.5	–	–	–	–
KF	18.2	17.6	15.5	16.1	13.5	14.1	11.8	12.3	10.2	10.7	8.8	9.3
RbF	27.2	26.1	23.9	24.9	21.8	22.7	19.8	20.7	18.1	18.9	16.6	17.3
CsF	38.8	37.4	35.2	36.6	33.2	34.5	31.3	32.6	29.6	30.9	28.2	29.4
AgF	8.6	7.5	5.9	6.9	4.5	5.5	3.2	4.2	1.5	2.4	–	0.7
AuF	5.8	4.7	3.4	4.5	2.8	3.8	0.9	2.0	–	0.7	–	0.2

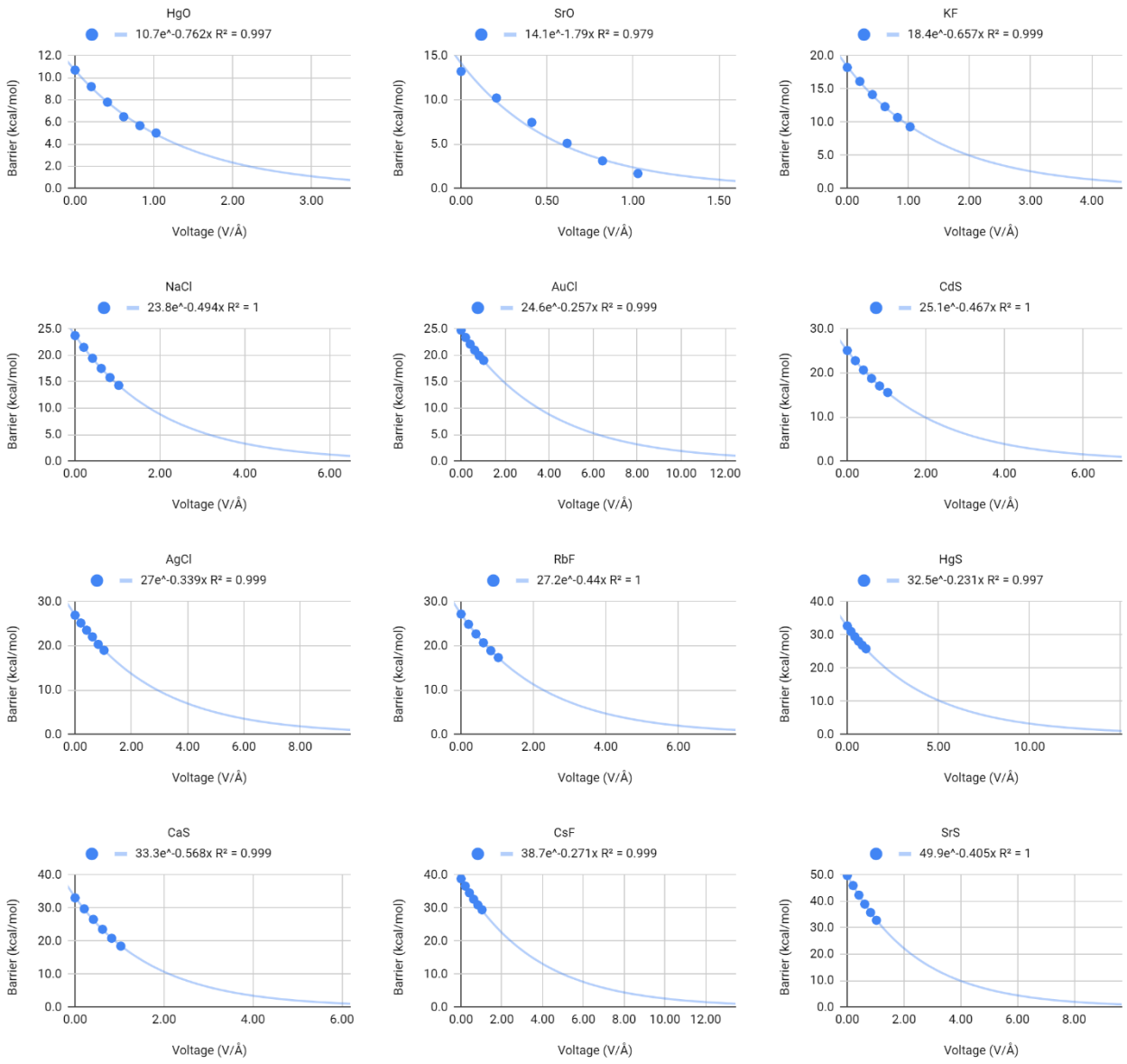

Figure S7: Extrapolations of the switching function (barrier-voltage dependence) of systems with intrinsic switching barrier between 10 and 50 kcal/mol. The blue points represent the barriers that were calculated at the PBE0-D3/def2-SVP level.

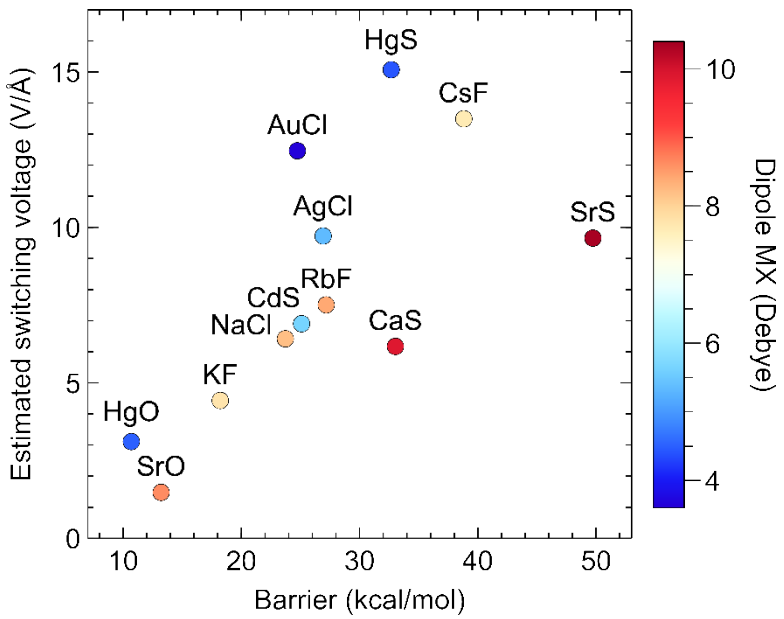

Figure S8: The correlation between the switching barrier, the estimated switching voltage, and the dipole moment of the free MX.

References

1. Helgaker T, Klopper W, Koch H, Noga J. Basis-set convergence of correlated calculations on water. J Chem Phys. 1997 Jun 15;106(23):9639–46.